Longitudinal Beam Dynamics of RF Voltage Modulation and Its Application

RF acceleration field has commonly been employed in advanced beam manipulations for various applications. When the sinusoidal rf phase or voltage modulation is applied to the rf system, the rf bucket is divided into stable islands produced by parametric resonance. Formation of islands within an rf bucket reduces the bunch density, peak current, and changes the frequency spectrum of the beam. In turns, beam lifetime and the threshold of beam instability may be improvd.

In the past few years, experimental measurements employing rf phase and voltage modulations have been carried out in many accelerator laboratories. However, systematic measurements of beam properties are limited, and theoretical description of these phenomena has remained within the framework of zero synchronous phase angle ϕ_s =0. In reality, the synchronous phase angle is non-zero in electron storage rings because of synchrotron radiation energy loss. The effect of non-zero synchronous phase angle has not been studied.

The rf voltage modulation changes the effective Hamiltonian of the particle motion, and thus modify the beam characteristics, e.g. the frequency spectrum of the beam. Thus some of the high order parasitic modes in rf cavity can be suppressed, which in turn may suppress the collective coupled bunch instability, and provide higher threshold beam current for scientific research.

This report describes the results of beam experiments performed at the Taiwan Light Source (TLS). These include applying rf voltage modulation to suppress multi-bunch collective beam instabilities and systematic studies of the resonance island bifurcation with rf voltage modulation. A more detailed report can be found in publication list.

The Hamiltonian of synchrotron motion, in the presence of rf voltage modulation, is given by

$$H = \frac{1}{2}\nu_s \delta^2 + \nu_s\{[1+\varepsilon \sin(\nu_m \theta+\xi)] [\cos\phi - \cos\phi_s] + (\phi - \phi_s)\sin\phi_s\}. \quad (1)$$

where ϕ and $\delta = -\frac{h|\eta|}{\nu_s}(\frac{\Delta p}{p_0})$ are conjugate phase space coordinates, the revolution angle $\theta = \omega_0 t$ serves as the independent variable, h is the harmonic number, η is the phase slip factor, $\nu_s = \sqrt{h|\eta| eV_{rf}/(2\pi\beta^2 E_0)}$ is the synchrotron tune at zero synchronous phase angle, p_0 and E_0 are the momentum and energy of a synchronous particle, $\Delta p = p - p_0$ is the momentum deviation, V_{rf} is the rf voltage, ε is the fractional rf voltage modulation amplitude, $\nu_m = f_m / f_0$ is the modulation tune, f_m is the modulation frequency, and $f_0 = \omega_0/2\pi$ is the revolution frequency of a synchronous particle. The synchronous phase angle ϕ_s is determined by the energy loss per revolution, i.e. $eV_{rf}\sin\phi_s = U(E_0)$. Where U is the radiation energy loss per-revolution.

The sinusoidal time dependent perturbation may produce parametric resonance islands near the center of the bucket and cause large perturbation to the Hamiltonian motion. We analyze the synchrotron motion at $\nu_m \approx 2\nu_s$ in Eq.(1). With two canonical transformations the new Hamiltonian becomes:

$$\bar{H} = \Delta J - \frac{1}{2}\alpha J^2 + GJ\cos(2\psi), \quad (2)$$

where (J,ψ) are conjugate phase-space coordinates, and the resonance proximity parameter Δ, nonlinear detuning parameter α, and the resonance strength G are given by

$$\Delta = (\nu_s|\cos\phi_s|^{1/2} - \frac{\nu_m}{2}), \quad (3)$$

$$\alpha = \frac{\nu_s}{8}(1 + \frac{5}{3}\tan^2\phi_s), \quad (4)$$

$$G = \frac{1}{4}\varepsilon\nu_s|\cos\phi_s|^{1/2}(1 + \frac{1}{3}\tan^2\phi_s), \quad (5)$$

The stable fixed points (SFP) of the Hamiltonian in Eq. (2) are

$$J_{sfp} = \begin{cases} \dfrac{24\nu_s|\cos\phi_s|^{1/2} - 12\nu_m + 2\varepsilon\nu_s|\cos\phi_s|^{1/2}(3+\tan^2\phi_s)}{\nu_s(3+5\tan^2\phi_s)}, & if\ \nu_m < \nu_{bif+}, \\ 0, & if\ \nu_m < \nu_{bif-}\ or\ \nu_m > \nu_{bif+}, \end{cases} \quad (6)$$

where

$$\nu_{bif+} = 2\nu_s|\cos\phi_s|^{1/2} + \frac{1}{2}\varepsilon\nu_s|\cos\phi_s|^{1/2}(1 + \frac{1}{3}\tan^2\phi_s), \quad (7)$$

$$\nu_{bif-} = 2\nu_s|\cos\phi_s|^{1/2} - \frac{1}{2}\varepsilon\nu_s|\cos\phi_s|^{1/2}(1 + \frac{1}{3}\tan^2\phi_s), \quad (8)$$

The unstable fixed points (UFP) are given by

$$J_{sfp} = \begin{cases} \dfrac{24\nu_s|\cos\phi_s|^{1/2} - 12\nu_m - 2\varepsilon\nu_s|\cos\phi_s|^{1/2}(3+\tan^2\phi_s)}{\nu_s(3+5\tan^2\phi_s)}, & if\ \nu_m < \nu_{bif-}, \\ 0, & if \nu_{bif+} > \nu_m > \nu_{bif-}, \end{cases} \quad (9)$$

This resonance corresponds to the nonlinear Mathieu instability. The formation of beamlets evolves as the modulation frequency is changed.

The TLS is a third generation light source. The rf cavities in the TLS storage ring are not higher-order-mode (HOM) free; multi bunch mode operation suffers coupled bunch collective instability due to a few strong parasitic modes. Fig. 1 shows a typical example of the collective beam instability observed from the images of streak-camera at 175.5 mA without rf voltage modulation. The top and bottom streaks in each graph show the images of the bunch numbers 1, 5, 9... and 3, 7, 11 ... respectively. The three graphs correspond to the images having a total time-span of 200 μs taken randomly at different time for an identical machine operation condition. Since a synchrotron period was about 40 μs, the time-span had about 5 synchrotron period. The 10 periods for the 200 μs time-span arises from quadrupole mode oscillations; the second graph from top became dominantly dipole mode; and the amplitude of dipole mode oscillation became much larger in the last graph. Although, the bunch motion appears regular for a short time interval

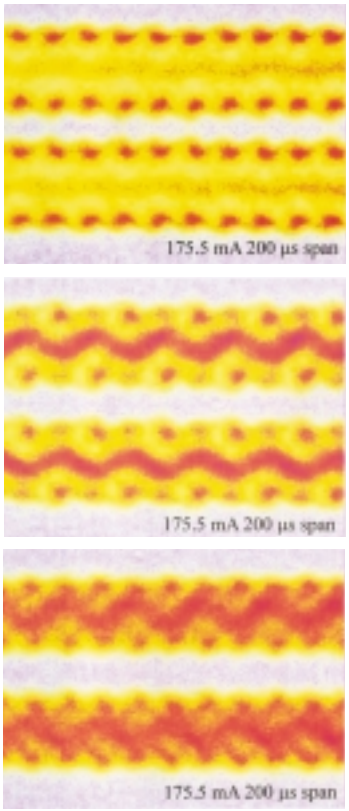

Fig. 1: Collective beam instability observed from images of streak-camera at 175.5 mA without rf voltage modulation. The images have a total time-span of 200 μs taken randomly at different time for an identical machine operational condition. The graphs taken at different times show different characteristic behaviors.

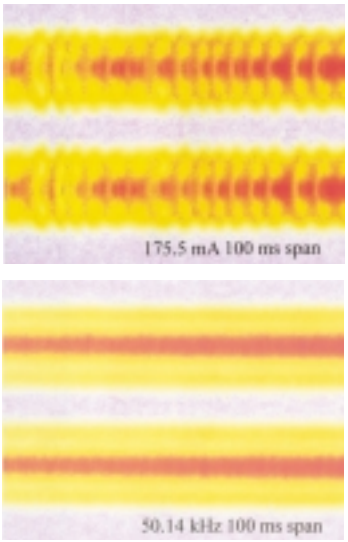

Fig. 2: The images of streak camera in a time-span of 100 ms. When rf voltage modulation with frequency 50.14 kHz was applied to the beam shown in the top graph, the beam became stable as shown in the bottom graph. This image corresponds to three beamlets rotate around the center of the bucket. See the bottom graph of Fig. 3 for a smaller time-span of 200 μs .

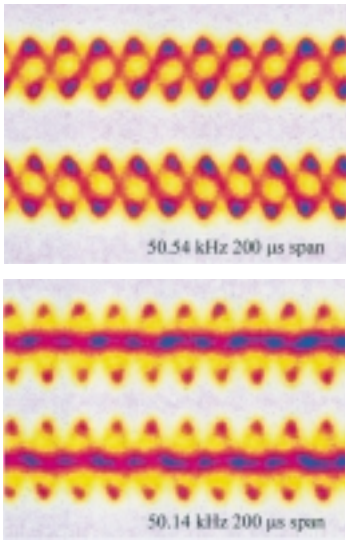

Fig. 3: Longitudinal motion of multi-bunch beam under rf amplitude modulation. The modulation frequencies were 50.54 kHz for the top graph and 50.14 kHz for the bottom graph. The modulation amplitude was 2.6% of the rf voltage. The full vertical was 1.4 ns and the horizontal scale was 200 μs . Note that the modulation frequency of the top graph was within f_{bif-} and f_{bif+} , and thus there existed only two beamlets. Since the modulation frequency in the bottom graph was below f_{bif-} , there were three beamlets in the bucket.

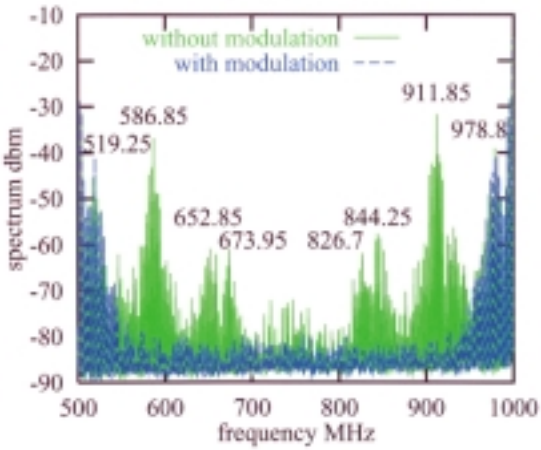

Fig. 4: Beam spectrum from BPM sum signal before and after applying rf voltage modulation. The modulation frequency was 50.155 kHz and the amplitude of modulation was 3.1%. The frequency span of the spectrum was 500 MHz.

within 200 μs, as observed in each of these three graphs, these graphs taken at different sampling times show different characteristic behaviors for a single store. The beam evidently encountered coupled bunch instability as shown in the top graph of Fig. 2, where the time-span of the streak-camera images is 100 ms.

We explored the feasibility of suppressing the coupled bunch instability with rf voltage modulations. The bottom graph of Fig. 2 shows an example of the beam images from the streak camera at an rf voltage modulation frequency 50.14 kHz in a time-span of 100 ms. Note that the modulation frequency was just below the bifurcation frequency f_{bif-}. In our experiments, it is found that the beam was most stable when the modulation frequency was set near the frequency f_{bif-} . The top plot of Fig. 3 shows the synchrotron oscillations of two beamlets in a time span of 200 μs at the modulation frequency of 50.54 kHz. The bottom plot of Fig. 3 shows synchrotron oscillations of three beamlets in a bucket at the modulation frequency of 50.14 kHz. This corresponds to a small time span in Fig. 2. The beamlets in all buckets rotate in phase because all bunches experience almost the same phase in the sinusoidal rf voltage modulation.

The beam stability in the presence of rf voltage modulation can also be measured from the beam spectrum. The beam spectrum can be obtained

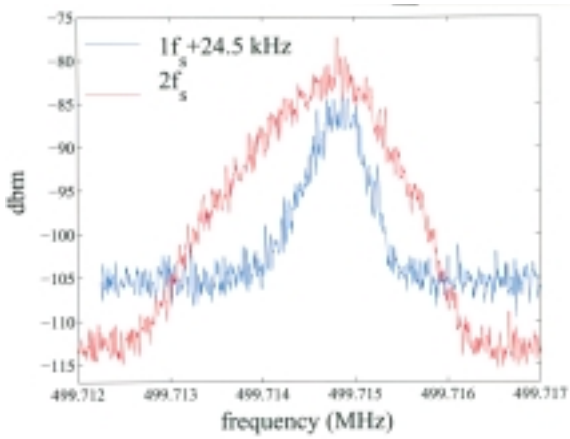

Fig. 5: The synchrotron sidebands at 1 f_s and 2 f_s are measured in the peak-hold mode to reveal the noise nature of the coupled-bunch instability. The spectra show the beam response to the perturbation induced by the wake field of the parasitic modes. The 1 f_s spectrum is shifted by 24.5 kHz to align with 2 f_s spectrum.

from a BPM sum signal using a spectrum analyzer. Fig. 4 shows the beam spectrum before (green) and after (blue) the rf voltage modulation for a conventional filling pattern of the stored beams in the TLS. Without rf voltage modulation, the beam spectrum shows characteristics of strong parasitic cavity modes. Once the beam is stabilized by the sinusoidal rf voltage modulation, the spectrum intensity of parasitic modes is highly suppressed.

To unravel the mechanism of collective beam instabilities, we carried out measurements of synchrotron sidebands during the onset of instabilities. Fig. 5 shows beam sideband spectra (of a primary revolution harmonic) at 1 f_s and 2 f_s in the peak-hold mode. Here, we observed that the synchrotron sidebands were randomly excited. In the peak-hold mode, the sideband spectra exhibit the response of the beam to the perturbation potential and its broadband nature (or narrowband at randomly excited frequencies). Based on the theory discussed in previous paragraphs, the peak of the 2 f_s sideband can be identified as f_{bif-}. At frequencies higher than f_{bif+}, the beam response should –become zero. The peak power of 2 f_s (circle) and the width (rectangles) are plotted as a function of the beam intensity in Fig. 6. Note that the threshold of beam instability is about 100 mA, and the width of the 2 f_s sideband (rectangles) increases from zero beyond the stability threshold.

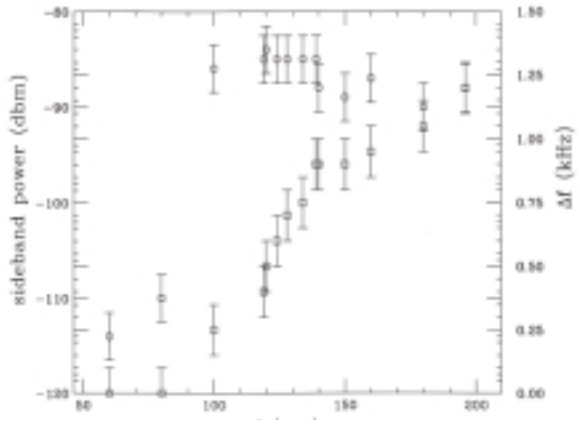

Fig. 6: The peak power of 2 f_s (circles) and the width $\triangle f = f_{bif+} - f_{bif-}$ (rectangles) are shown as a function of the beam current. Note that the threshold current for the instability is about 100 mA.

The rf voltage modulation produced a dominant impact on the beam spectrum. Fig. 7 shows the 2 f_s synchrotron sideband in the peak-hold mode as the frequency of the voltage modulation is scanned across the 2 f_s sideband. We note that the noise spectrum is dramatically suppressed when the modulation frequency reaches the f_{bif-}. When all particles are forced to make coherent synchrotron oscillation, the noise spectrum will be suppressed. This will occur when the resonance island created by the rf voltage modulation is large enough to contain all particles in a bunch.

These results indicate that the parasitic cavity

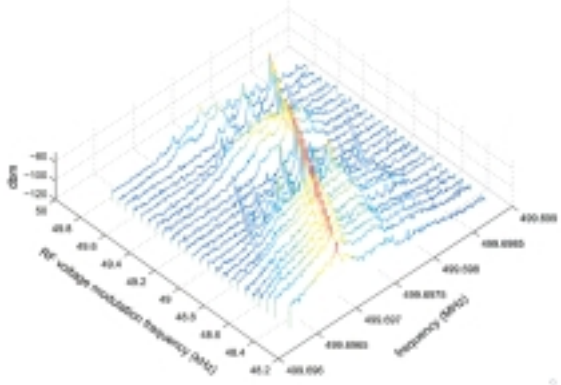

Fig. 7: The observed 2 f_s synchrotron sideband power spectrum (in the unit of dBm) for a sum signal in the peak-hold mode for the TLS at 190 mA, nearly uniformly distributed in 160 bunches. Note that the 2 f_s sideband induced by wake field is highly suppressed when the modulation frequency was about 49.2 kHz.

modes were excited by the noise spectrum of the beam. When the rf amplitude modulation with an appropriate modulation tune is applied to the rf system, each bunch may split into two or three beamlets; this process can suppress noise harmonic near parasitic mode frequencies. Once the beam motion is stabilized by the coherent rf voltage modulation, there is no beam power near the parasitic frequency and thus the beam power at these parasitic mode frequencies is suppressed. Since the bunch shape rotates at the modulation frequency f_m, it does not affect the stability of photon beam except a small reduction of photon beam brilliance due to a large effective beam size.

We developed a theoretical description of rf voltage modulation on synchrotron motion with a non-zero synchrotron phase angle. The coupled bunch instability observed at the TLS shows the transient characteristics of rigid dipole and quadrupole mode oscillations (see the graphs in Fig. 2). The frequency spectrum of an unstable beam exhibits strong parasitic mode excitation of the rf cavities. The sinusoidal rf voltage modulation has been shown to effectively suppress collective beam instabilities in the Taiwan Light Source.

Authors:

M. H. Wang

Synchrotron Radiation Research Center, Hsinchu, Taiwan

S. Y. Lee

Department of Physics, Indiana University

Publications:

- M. H. Wang, S. Y. Lee, J. Appl. Phys. **92**, 555 (2002).
- M. H. Wang, S. Y. Lee, Asia Particle Accelerator Conference, Beijing, China, September 17-21, 2001.
- M. H. Wang, Peace Chang, J. P. Chou, K. T. Hsu, C. C. Kuo, J. C. Lee, W. K. Lau, Proceeding of Particle Accelerator Conference PAC99, 2837 (1999).
- M. H. Wang, L. H. Chang, Peace Chang, K. T. Hsu, C. S. Hsue, C. C. Kuo, W. K. Lau, Proceeding of Particle Accelerator Conference PAC97, 1487 (1997).